Am J Cancer Res 2019;9(11):2379-2396
www.ajcr.us /ISSN:2156-6976/ajcr0101829

Original Article

Akt inhibition at the initial stage of CAR-T preparation enhances the CAR-positive expression rate, memory phenotype and in vivo efficacy

Qing Zhang[1,2*], Jiage Ding[1,2*], Shishuo Sun[1,2], Hongyan Liu[1,2,3], Mengmeng Lu[1,2], Xiaohuan Wei[1,2], Xiaoge Gao[1,2], Xiaokang Zhang[1,2], Qiang Fu[4], Junnian Zheng[1,2]

[1]Cancer Institute, Xuzhou Medical University, Xuzhou, Jiangsu, P. R. China; [2]Center of Clinical Oncology, Affiliated Hospital of Xuzhou Medical University, Xuzhou, Jiangsu, P. R. China; [3]The Second People's Hospital of Lianyungang, Lianyungang, Jiangsu, P. R. China; [4]Department of Immunology, Binzhou Medical University, Yantai, Shandong, P. R. China. [*]Equal contributors.

Received September 3, 2019; Accepted October 12, 2019; Epub November 1, 2019; Published November 15, 2019

Abstract: The adoptive transfer of chimeric antigen receptor-modified T (CAR-T) cells is a novel cancer treatment that has led to encouraging breakthroughs in the treatment of haematological malignancies. The efficacy of infused CAR-T cells is associated with a high CAR-positive expression rate, a strong proliferative response and the persistence of CAR-T cells in vivo. Manufacturing CAR-T cells is a process usually associated with the decreased CAR-positive expression rate and terminal differentiation of the infused CAR-T cells, which causes decreased proliferation and persistence of CAR-T cells in vivo. Therefore, the preparation of a high CAR-positive expression rate and few differentiated CAR-T cells is particularly important for clinical cancer treatment. In this study, we transduced and expanded CAR-T cells targeting the epithelial cell adhesion molecule (EpCAM) in the presence of an Akt inhibitor (MK2206) during the initial stage of CAR-T cell preparation. We show that the Akt inhibitor did not suppress the proliferation or effector function of the EpCAM-CAR-T cells but increased the CAR-positive expression rate and decreased the number of terminally differentiated EpCAM-CAR-T cells. Furthermore, EpCAM-CAR-T cells prepared using this protocol appeared to have enhanced antitumor activity in vivo. Taken together, these findings suggest that Akt inhibition during the initial stage of CAR-T cell preparation could improve the performance of CAR-T cells.

Keywords: CAR-T, Akt inhibitor, MK2206, CAR-positive expression rate, memory phenotype

Introduction

The adoptive transfer of chimeric antigen receptor-modified T (CAR-T) cells is a novel cancer treatment that has achieved encouraging breakthroughs in the treatment of haematological malignancies. The efficacy of infused CAR-T cells is associated with a high CAR-positive expression rate, a strong proliferative response and the persistence of the gene-modified T cells in vivo [1]. Manufacturing CAR-T cells is a process that involves activation ex vivo, CAR gene transfer and expansion in culture, where these cells grow to a suitable number for therapeutic use. However, this process is usually associated with a decreased CAR-positive expression rate and suppressed proliferation and persistence in vivo [2].

The CAR-positive expression rate is determined by gene transduction and expression efficiency. Lentivirus or retroviral infection is the most commonly used gene transduction methods for preparing CAR-T cells [1]. Both are derived from the human immunodeficiency virus-1 (HIV-1). The infection efficiency of HIV is modulated by the state of the host cell cycle. Cell cycle arrest in G2/M can promote the early steps of HIV infection [3, 4]. In addition, the results of previous research showed that the degree of G2/M suppression was positively correlated with the gene expression efficiency of the infected lentivirus [5]. An extended G0/G1 phase can promote HIV-1 gene expression, which is important for improving the ability of lentivirus vectors to enter host cells and efficiently express the gene of interest [6, 7].

Inhibiting the Akt pathway can cause cell cycle arrest at G0/G1 or G2/M. Pristimerin, an active compound isolated from the traditional Chinese herbs Celastraceae and Hippocrateaceae, induces G1 phase arrest by inhibiting Akt signalling [8]. Overexpressed desmocollin 3, a transmembrane adhesion protein of desmosomes, induced G0/G1 cell cycle arrest through inhibition of the Akt pathway in colorectal cancer cells [9]. Overexpressed inhibitor of growth 3, a tumor-suppressor gene, induced cell cycle arrest in G2/M by blocking the Akt pathway in gastric cancer cells [10]. DCZ3301, an aryl-guanidino inhibitor, induced cell cycle arrest in G2/M by suppressing the Akt pathway of T-cells in leukaemia/lymphoma [11]. Together, these results demonstrate that Akt pathway inhibition can induce cell cycle arrest in G0/G1 or G2/M. However, whether Akt inhibitors increase the CAR-positive expression rate by disrupting the cell cycle is not known.

Terminally differentiated infused CAR-T cells have decreased proliferation and persistence in vivo [1, 12]. Infusion of less-differentiated CAR-T cell subsets is associated with greater tumor regression [13, 14]. However, physiologically, the expansion and differentiation processes of CAR-T cells are closely linked. Several studies have indicated the importance of the Akt pathway in the regulation of T cell differentiation and memory formation [15-17]. Once the T cell surface receptors, co-stimulatory molecules, and/or cytokine receptors are induced, the PI3K-Akt pathway is activated, resulting in downstream responses via the phosphorylation of a range of intracellular proteins and T cell activation. However, studies have confirmed that sustained Akt activation progressively drives T cells towards terminal differentiation and decreased antitumor activities [15].

Based on these findings, we speculated that inhibited Akt activity during CAR-T cell preparation may enhance the CAR-positive expression rate and enhance the memory phenotype of CAR-T cells. To confirm this speculation, we transduced and expanded CAR-T cells targeting epithelial cell adhesion molecule (EpCAM) in the presence of an Akt inhibitor (MK2206) during the initial stage of CAR-T cell preparation. We show that Akt inhibition did not suppress proliferation or effector function but increased the CAR-positive expression rate and inhibited the terminal differentiation of the EpCAM-CAR-T cells. Furthermore, the EpCAM-CAR-T cells that expanded in the presence of Akt inhibitor MK2206 appeared to have enhanced antitumor activity in vivo. Taken together, these findings suggest that Akt inhibition during the initial stage of CAR-T preparation could improve the performance of CAR-T cells.

Materials and methods

Cell culture

Human colon cancer cell lines (HCT116 and SW620) and 293T cells were maintained in Dulbecco's modified Eagle's Medium (DMEM, Gibco, USA) supplemented with 10% foetal bovine serum (Gibco, USA) and 1% penicillin/streptomycin (Gibco, USA). Luciferase-expressing HCT116 cells were generated by transduction of the colon cancer cell line HCT116 with lentiviral particles encoding the Luciferase sequence. T cells were cultured in X-vivo 15 medium (Lonza, Switzerland) supplemented with 10% FBS and 200 IU/mL recombinant human interleukin-2 (rhIL-2) (Shuanglu Pharmacy, Beijing China). All cells were incubated at 37°C in a 5% CO_2 humidified atmosphere.

Generation of EpCAM-CAR-T cells

Human peripheral blood mononuclear cells (PBMCs) were obtained from healthy donors using a Ficoll gradient (Axis-Shield, Norway), centrifuged and frozen in liquid nitrogen. When preparing the CAR-T cells, the thawed PBMCs were activated with CD3/CD28 Dynabeads (Gibco, USA) at a ratio of 1:1. Two days after stimulation, the cells were transduced with a lentivirus encoding a CAR targeting EpCAM with a co-stimulatory molecule, 4-1BB, at a multiplicity of infection (MOI) of 5 and expanded in medium containing 200 IU/mL rhIL-2 and 0-4 μM Akt inhibitor (MK2206, Selleck). Five days later, Dynabeads and the MK2206 were removed, and the lentivirus-infected T cells were continuously expanded for another 5-9 days. Then, expanded CAR-T cells were used for experiments in vitro or in vivo.

Flow cytometry

Single cell samples were incubated with live/dead green dye (L23101, Life Technologies, USA) and the indicated antibodies or isotype

controls in staining buffer (PBS containing 2% FBS) for 30 mins at 4°C and then fixed in 1% paraformaldehyde. Fluorescence data were collected on a FACS machine (FACS Canto II, Becton-Dickinson, USA). Data analysis was performed using FlowJo 10 software (Ashland, OR). To determine CAR expression at the end of CAR-T cell expansion (Day 10), 2×10^5 T cells were stained, first with a mouse anti-c-myc tag monoclonal antibody (Sigma-Aldrich, USA) and, then, with an Alexa Fluor 647-conjugated goat anti-mouse IgG (H+L) secondary antibody (Thermo Fisher, USA). For p-Akt determination, intracellular staining was performed with FITC-conjugated anti-p-Akt (s473) (eBioscience, USA). To determine EpCAM expression, cell samples were stained with Alexa Fluor 647-conjugated anti-human EpCAM (Biolegend, USA). For the determination of other immune cells, the cells were stained with anti-human CD3-PerCP, CD45-FITC, CD45RA-PE-Cy7, CCR7-APC-Cy7, Low-density lipoprotein receptor (LDL-R)-AlexaFluor 488 (R&D system, USA) and their respective isotype control antibodies. In addition to antibodies against LDL-R, other antibodies and their respective isotype controls were purchased from Biolegend. For CAR-T cell determination in peripheral blood, 50 μL of blood was drawn from the tail vein of mice. These red blood cells were lysed by hypotonic lysis using 1 × RBC lysis buffer (PeproTech, USA) in a dark at room temperature for 10 mins. Total leukocytes were collected and stained with anti-human CD45 and CD3 antibodies.

Western blot analysis

For Akt, p-Akt and LDL-R detection, cells were lysed and maintained on ice for 30 mins in RIPA buffer with 1 × protease inhibitor cocktail and 0.5 mM PMSF. After centrifugation at 12000 rpm at 4°C for 15 mins, the protein concentration of the supernatant was determined using a BCA kit (Beyotime, China). An anti-Akt (pan) rabbit mAb (Cell Signaling Technology, USA), anti-p-Akt (Ser473) rabbit mAb (Cell Signaling Technology, USA) and anti-LDL receptor rabbit monoclonal antibody (Abcam, UK) were used to detect pan Akt, p-Akt and LDL-R, respectively. Anti-GAPDH antibody (Santa Cruz Biotechnology, USA) was used to detect GAPDH, which was the internal control. For the detection of FoxO1 in the cytoplasm and nucleus, nuclear and cytoplasmic proteins were extracted according to the manufacturer's instructions that came with the nuclear and cytoplasmic protein extraction kit (Beyotime, Suzhou, China). Anti-FoxO1 Rabbit mAb (Cell Signalling Technology, USA) was used to detect FoxO1 in the nucleus and cytoplasm. Anti-PARP antibody (Santa Cruz Biotechnology, USA) was used to detect PARP in the nucleus as an internal control. Anti-β-tubulin antibody (Santa Cruz Biotechnology, USA) was used to detect β-Tubulin in the cytoplasm, which was the internal control. The intensity of each strip was analyzed by ImageJ software. The average intensities of each protein were standardized to its internal reference.

Confocal immunofluorescence imaging

For immunofluorescent staining, cells were fixed with 4% paraformaldehyde and incubated with primary anti-FoxO1 (C29H4) rabbit mAb (Cell Signaling Technology, USA). Then, the antigen was probed with an Alexa Fluor 488-conjugated goat anti-rabbit IgG (HL) antibody (Abcam, UK). Hoechst 33342 counterstain was used to mark the nucleus. The images were taken with a confocal microscope.

Cell cycle analysis

Human PBMCs were activated with CD3/CD28 Dynabeads in medium containing 2 μM MK2206 or a vehicle control for 48 h. Cells were washed with PBS and fixed in 2 mL of ice-cold 70% ethanol overnight. Then, the cells were stained with propidium iodide solution containing 0.1% Triton X-100 and 0.2 mg/mL RNase (Beyotime, China). Populations in cell cycle phases were quantified by FACS Canto II.

Cytokine release analysis by ELISA

Target cells were co-cultured with effector cells at a 1:1 ratio (1×10^4 cells each) in U-bottom 96-well plates with 100 μL of medium in triplicate. After 24 h, the culture supernatant was collected through centrifugation at 300 g for 5 mins. The cytokine levels (IFN-γ and granzyme B) were quantified using a human ELISA kit according to the manufacturer's instructions (BD Biosciences, USA).

Real-time cell assay (RTCA)

The cytotoxic activity of CAR-T cells was determined using an xCELLigence RTCA MP instru-

ment (ACEA Biosciences, USA). First, 50 μL of target cell culture media was added to each well of a 2 × 8-well E-Plates (ACEA Biosciences, USA), and then, the background impedance was measured and used as the cell index. Then, target cells were seeded at a density of 10000 cells/well of the E-Plate in a volume of 100 μL and allowed to passively adhere on the electrode surface. Post-seeding, the E-Plate was kept at ambient temperature inside a laminar flow hood for 30 mins and then transferred to the RTCA MP instrument inside a cell culture incubator. Data recording was initiated immediately at 15-minute intervals for the entire duration of the experiment. After approximately 10 h, the target cells reached a logarithmic growth phase, and the effector cells were added at an effector/target (E:T) ratio = 1:1, in duplicate, in a volume of 50 μL. After transferring the E-Plate back into the xCELLigence system, data acquisition was resumed to monitor the CAR-T cell cytotoxic activity based on the viability of the attached target cells, which is reflected by cell index values.

Therapeutic efficacy in vivo

Six-week-old male NPG (NOD-Prkdc^{scid} Il2rg^{null}) mice (Vitalstar Biotechnology, Beijing, China) were maintained in the specific pathogen-free animal facilities of the Experimental Animal Center of Xuzhou Medical University. All animal procedures were approved by and manipulated in accordance with the Institutional Ethical Care and Use Committee. For metastasis models, each mouse was injected intravenously through the tail vein with 1 × 10^6 HCT116 cells with a luciferase-expressing gene (HCT116^{Luc+}). Seven days later, the mice were randomly assigned to 2 groups (n = 5): vehicle-treated CAR-T (Vehicle) and MK2206-treated CAR-T (MK2206). A total of 3 × 10^6 vehicle-treated CAR-T cells or MK2206-treated CAR-T cells were injected intravenously (i.v.) into the mice. All mice were intraperitoneally (i.p.) administered IL-2 (2000 IU/mouse) daily during the treatment. After two weeks of treatment, 50 μL of blood was obtained through the tail vein and used to determine the proliferation of the transfused CAR-T cells. After three weeks of treatment, 150 mg/kg D-luciferin (Sigma-Aldrich, USA) was injected intraperitoneally into the mice. The tumor burden was evaluated through luminescence imaging with an IVIS system (Berthold Technologies, Germany). The survival of the mice was also assessed. The death of the mice was recorded throughout the course of treatment. At the end of the treatment, survival curves of the mice were plotted, and the therapeutic effects of the CAR-T cells were evaluated.

Statistical analysis

Data were analysed and plotted with GraphPad Prism software (GraphPad, San Diego, CA, USA) and are presented as the mean ± SEM. All comparisons except for in vivo experiments between two groups were performed by unpaired two-tailed Student's t test. Wilcoxon test was applied for the comparison of in vivo experiments. $P < 0.05$ was considered significant.

Results

MK2206 significantly inhibits Akt phosphorylation in the initial stage of T cell activation

The construction and characteristics of a second-generation CAR that targets EpCAM are presented in **Figure 1A** and explained in our previous report [18]. The DNA sequence of the CAR was inserted into a second-generation lentiviral vector system, pRRL. To simulate the source of the T cells used in the majority of current CAR-T clinical trials [19-21], we used an unfractionated population of peripheral blood mononuclear cells (PBMC). To determine whether MK2206-inhibited Akt phosphorylation could enhance the performance of EpCAM-CAR-T cells, we performed T cell stimulation and lentiviral transduction of EpCAM-CAR in the continuous presence of 0.5 μM, 1 μM, 2 μM, or 4 μM MK2206 or a vehicle control. After 5 days of treatment, the MK2206 and anti-human CD3/CD28 beads were removed from the medium (**Figure 1B**).

After two, five or ten days of expansion ex vivo, intracellular phosphorylation of Akt (p-Akt) in the T cells was analysed by flow cytometry. We found that at all concentrations, MK2206 significantly inhibited Akt phosphorylation in bead-activated T cells on day 2, and compared with the CAR-T cells treated with different concentrations of MK2206, the positive rate of p-Akt decreased from 53% of the vehicle to approximately 6%. On day 5, the overall phosphorylation levels of Akt in the EpCAM-CAR-T cells that

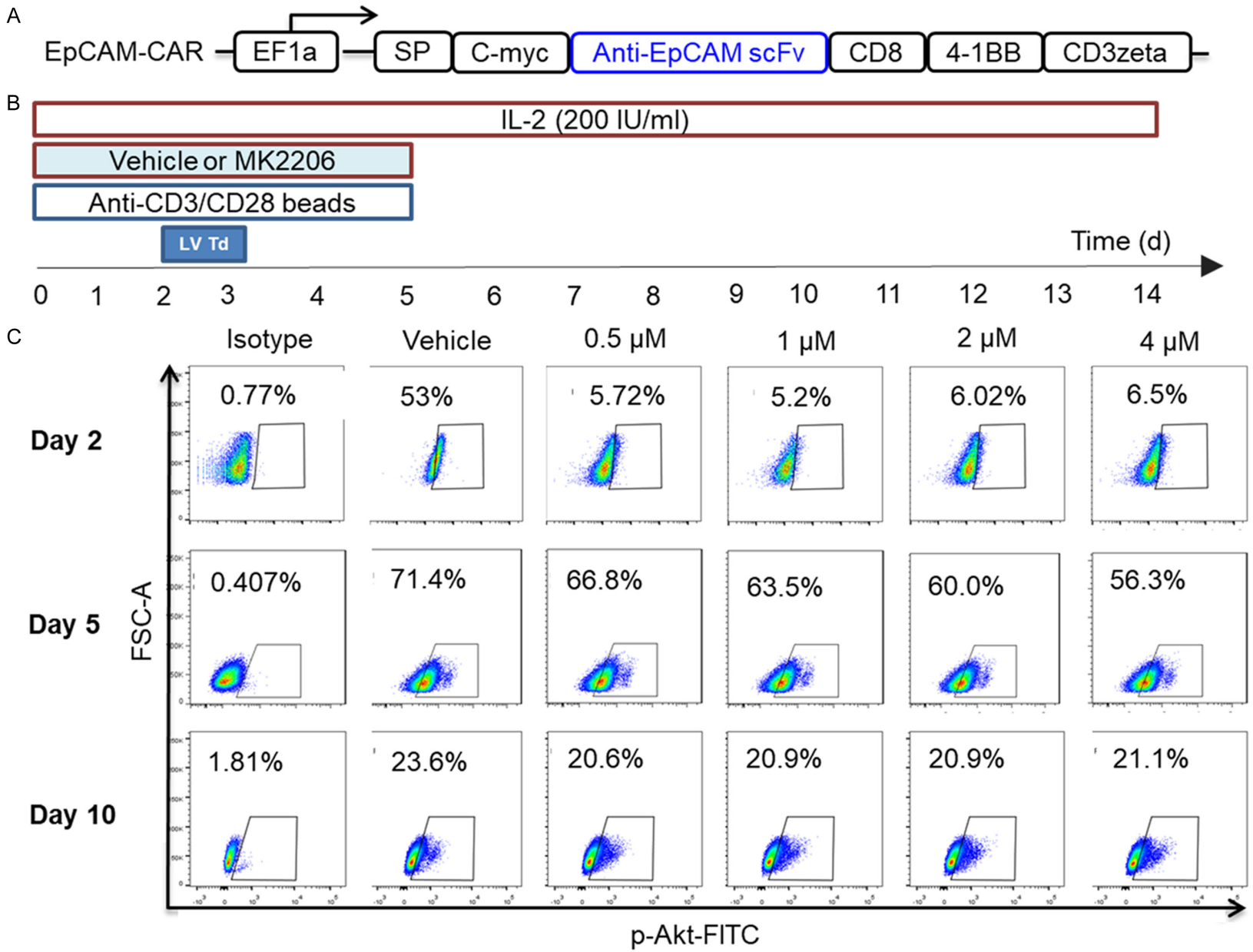
A
EpCAM-CAR
EF1a
SP
C-myc
Anti-EpCAM scFv
CD8
4-1BB
CD3zeta
B
IL-2 (200 IU/ml)
Vehicle or MK2206
Anti-CD3/CD28 beads
LV Td
Time (d)
0 1 2 3 4 5 6 7 8 9 10 11 12 13 14
C
Isotype
Vehicle
0.5 μM
1 μM
2 μM
4 μM
Day 2
Day 5
Day 10
0.77%
53%
5.72%
5.2%
6.02%
6.5%
0.407%
71.4%
66.8%
63.5%
60.0%
56.3%
1.81%
23.6%
20.6%
20.9%
20.9%
21.1%
FSC-A
p-Akt-FITC

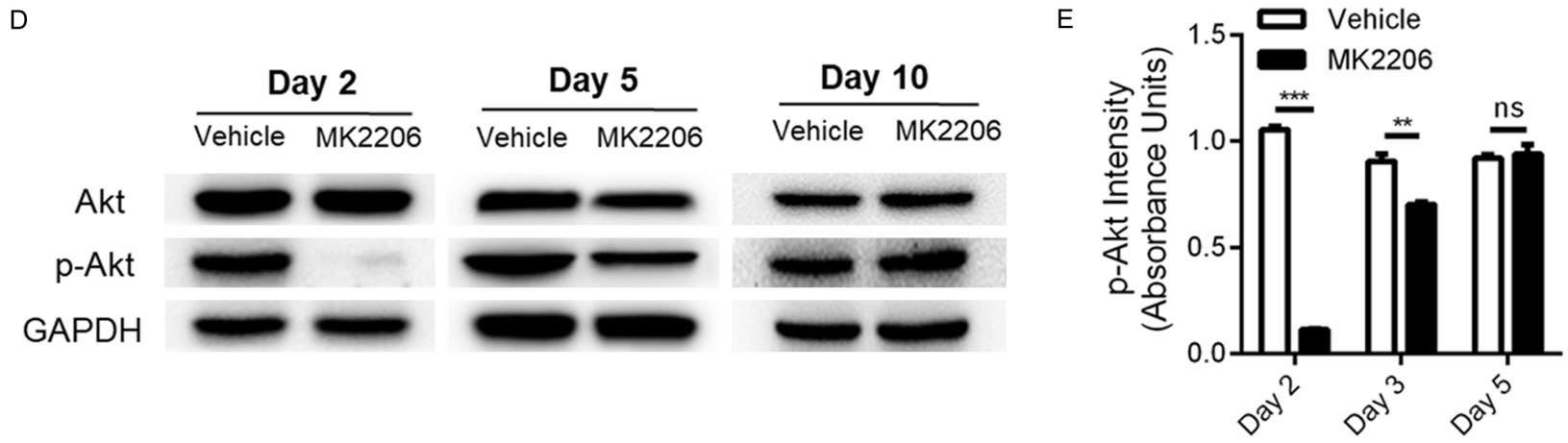

Figure 1. The Akt inhibitor MK2206 significantly suppresses Akt phosphorylation at the initial stage of CAR-T cell preparation. A. Schematic illustration of EpCAM-specific CAR. Sequences encoding EpCAM-scFv with a c-myc tag at the N-terminus were fused with the transmembrane domain of human CD8α and the cytoplasmic regions of 4-1BB and CD3ζ. EF1α: promoter; SP: signal peptide; scFv: single-chain variable fragment. B. Schematic diagram of CAR-T cell preparation. PBMCs were activated with CD3/CD28 Dynabeads in medium containing 200 IU/mL rhIL-2 and a vehicle control or 0.5-4 μM Akt inhibitor MK2206. Two days later (day 2), the activated cells were transduced with a lentivirus encoding EpCAM-specific CAR (MOI = 5). Five days later (day 5), Dynabeads and the MK2206 were removed, and the lentivirus-infected T cells were continuously expanded for another 5-9 days. LV Td, lentivirus transduction. C. The inhibitory effects of MK2206 on Akt phosphorylation in T cells were detected by flow cytometry. T cells treated with MK2206 or the vehicle were collected on days 2, 5 and 10 and intracellularly stained with antibodies against phosphorylated Akt (p-Akt). D. The inhibitory effects of MK2206 on Akt phosphorylation in T cells as detected by western blotting. T cells treated with MK2206 or the vehicle were collected on days 2, 5 and 10. Total proteins were extracted. Pan Akt and p-Akt were detected with antibodies against Akt and p-Akt, respectively. GAPDH was also detected as the internal control. E. The quantitative analysis results of p-Akt in the western blot analysis. The intensity of each strip was analyzed by ImageJ software. The average intensities of p-Akt were standardized to GAPDH. Shown are combined data from 3 independent experiments with mean ± SEM. **P < 0.01; ***P < 0.001; ns, not significant.

had been treated with MK2206 at different concentrations increased; however, the efficiency of the MK2206 inhibition decreased. The positive rate of p-Akt decreased from 71.4% of the vehicle to 56.3% of the cells treated with 4 μM MK2206. Five days after the activating beads and MK2206 were removed (Day 10), the positive rate of p-Akt in EpCAM-CAR-T cells was reduced to approximately 21%. There was no significant difference between CAR-T cells treated with the vehicle and those treated with different concentrations of MK2206 (**Figure 1C**). To further confirm the inhibition of Akt phosphorylation, the intracellular p-Akt in the T cells treated with the vehicle or 2 μM MK2206 on days 2, 5 and 10 were analysed by western blotting. We consistently found that 2 μM MK2206 resulted in almost complete inhibition of Akt phosphorylation in bead-activated T cells on day 2, and the total Akt was unaltered. However, the efficiency of this inhibition decreased by day 5 and completely disappeared by day 10 (**Figure 1D** and **1E**). These data demonstrate that MK2206 can significantly inhibit Akt phosphorylation during the initial stage of CAR-T cell preparation.

Akt inhibition generates an EpCAM-CAR-T cell population with an enhanced CAR-positive expression rate

To investigate the effects of MK2206-induced Akt inhibition on the CAR-positive expression rate, the expression of EpCAM-CAR in the T cells treated with the vehicle or with different concentrations of MK2206 on day 7 and day 14 was analysed with flow cytometry and an anti-C-myc tag antibody. We found that MK2206 treatment resulted in a significant increase in the CAR-positive expression rate compared with the vehicle on both day 7 (from 14.2% to 31.9%) and day 14 (from 10.6% to 32.7%). Furthermore, the increased CAR-positive expression rate was dose-dependent. The CAR-positive expression rate of EpCAM-CAR-T cells treated with 2 μM MK2206 was approximately 2-fold that of cells treated with the vehicle on both day 7 and day 14 (**Figure 2A** and **2B**). These data demonstrated that MK2206-inhibited Akt phosphorylation generates an EpCAM-CAR-T cell population with an enhanced CAR-positive expression rate.

Previous studies have shown that inhibition of the Akt pathway can cause cell cycle arrest in G0/G1 or G2/M [8-11], which has important implications for enhancing the ability of lentiviral vectors to enter host cells and the expression efficacy of interest genes [6, 7]. To verify whether MK2206 increases the CAR-positive expression rate by disrupting the cell cycle, after 2 μM MK2206 treatment for 2 days during expansion ex vivo, the cell cycle of the bead-activated T cell populations was analysed with flow cytometry. As shown in **Figure 2C** and **2D**, the MK2206 treatment caused significant cell cycle arrest in the G0/G1 and G2/M phases.

Another factor affecting the infection efficiency of lentivirus is the expression level of the virus receptor in host cells. The lentiviruses used in this study were prepared with the envelope plasmid encoding vesicular stomatitis virus glycoprotein (VSVG). Low-density lipoprotein receptor (LDL-R), which is ubiquitously expressed in many human cell types, is required by lentivirus with a VSVG envelope for cell entry [22]. To confirm whether MK2206 treatment increased the expression level of LDL-R, thereby enhancing the infection efficiency of lentivirus, we analysed the expression of this receptor in bead-activated T cells that were treated for 2 days with the vehicle or MK2206 (2 μM) by flow cytometry (**Figure 2E** and **2F**) and western blotting (**Figure 2G**). However, we observed that MK2206 neither induced an increase in LDL-R expression level nor induced a decrease in the expression level of bead-activated T cells. Therefore, the nature of the available receptor did not limit the transduction of the lentivirus, and the increased CAR-positive expression rate caused by MK2206 treatment is not due to the upregulation of LDL-R expression. Together, these data indicated that MK2206 may enhance the EpCAM-CAR-positive expression rate by causing cell cycle arrest in the G0/G1 and G2/M phases rather than through LDL-R expression.

MK2206 treatment generates EpCAM-CAR-T cell populations with memory-like characteristics

Previous studies showed that CAR-T cells with terminal differentiation status have decreased proliferation and persistence in vivo [1, 12], and infusion of early differentiated T cells show significant survival advantages over terminally differentiated T cells in vivo [23]. Currently, CAR-T cells are usually prepared through activa-

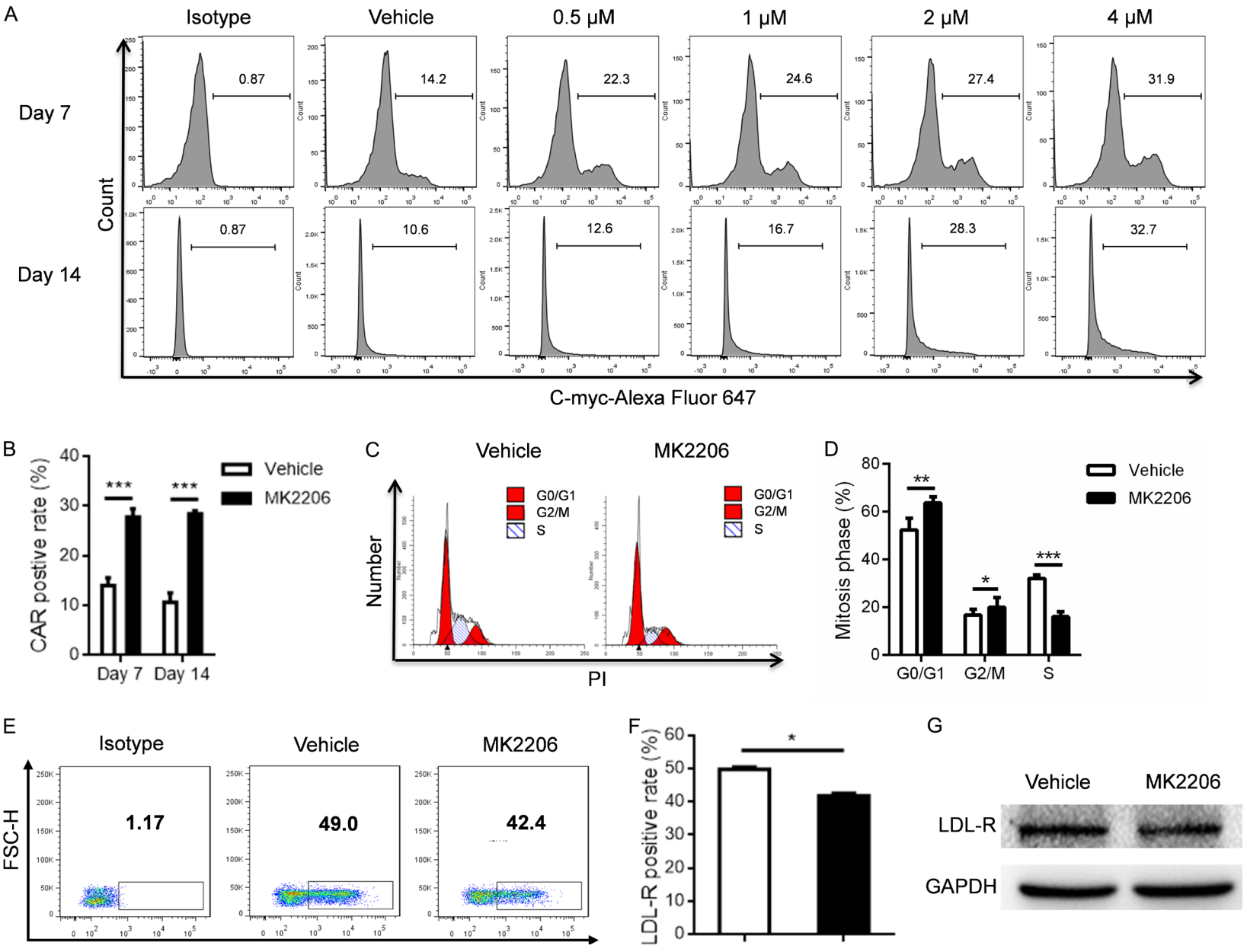
A
Isotype
Vehicle
0.5 μM
1 μM
2 μM
4 μM
Day 7
Day 14
Count
0.87
14.2
22.3
24.6
27.4
31.9
0.87
10.6
12.6
16.7
28.3
32.7
C-myc-Alexa Fluor 647
B
CAR postive rate (%)
Vehicle
MK2206
***
***
Day 7
Day 14
C
Vehicle
MK2206
G0/G1
G2/M
S
Number
PI
D
Mitosis phase (%)
Vehicle
MK2206
**
*
***
G0/G1
G2/M
S
E
Isotype
Vehicle
MK2206
FSC-H
1.17
49.0
42.4
F
LDL-R positive rate (%)
*
G
Vehicle
MK2206
LDL-R
GAPDH

Figure 2. Akt inhibition enhanced the CAR-positive expression rate of EpCAM-CAR-T cells through cell cycle arrest rather LDL receptor expression. (A) Representative data of CAR expression were detected by flow cytometry. The EpCAM-specific CAR-T cells were prepared as described in **Figure 1B**, with treatment with the vehicle or 0.5~4 μM MK2206. CAR-T cells were collected on days 7 and 14. CAR expression was detected by flow cytometry with an anti-c-myc tag antibody and an Alexa Fluor 647-conjugated second antibody. (B) Statistical results of the CAR expression in CAR-T cells treated with the vehicle or 2 μM MK2206 on day 7 and day 14. (C, D) Representative and statistical data of the cell cycle analysis of MK2206-treated T cells by flow cytometry. PBMCs were activated with CD3/CD28 Dynabeads in medium containing 200 IU/mL rhIL-2 and a vehicle or 2 μM MK2206. Two days later, the cell cycle of the T cells was analysed by flow cytometry. (E, F) Determination of LDL receptor (LDL-R) expression by flow cytometry. The vehicle or MK2206-treated T cells were incubated with a mouse anti-human LDL-R monoclonal antibody or isotype control antibody and subsequently stained with an Alexa Fluor 488-conjugated goat anti-mouse secondary antibody. Representative data (E) and quantitative results (F) are shown. n = 3. (G) The LDL-R expression was determined by western blotting. Total proteins were extracted from the vehicle or MK2206-treated T cells. The LDL-R was detected with the mouse anti-human LDL-R monoclonal antibody. GAPDH was also detected as the internal control. The results showed a consistent trend. Shown are combined data from 3 independent experiments with mean values ± SEM. *P < 0.05; **P < 0.01; ***P < 0.001.

tion with CD3/CD28 beads and expanded with the support of the cytokine IL-2 [24]. However, during this process, the PI3K-Akt-mTOR pathway is continuously activated because of persistent stimulation, which leads to the terminal differentiation of CAR-T cells [25].

To verify whether inhibition of Akt phosphorylation generates fewer differentiated CAR-T cells, PBMCs were activated, infected and expanded in medium containing 0-4 μM MK2206 in the first 5 days (**Figure 1B**). On days 7 and 14, the memory phenotype of the CAR-T cells was analysed by flow cytometry with anti-CCR7 and anti-CD45RA antibodies. As shown in **Figure 3A**, the MK2206 treatment resulted in a significant increase in the central memory T cells (T_{CM}, $CCR7^+$ $CD45RA^-$) and $CCR7^+$ $CD45RA^+$ cell populations compared with vehicle treatment on days 7 and 14. The $CCR7^+$ $CD45RA^+$ cell population in this system was further confirmed to be $CD95^+$ $CD27^+$ $CD62L^+$ T memory stem cells (T_{SCM}, data not shown). Furthermore, the increase was dose-dependent. Specifically, the memory phenotype of the CAR-T cells treated with 2 μM MK2206 was analysed. We found that, on day 7, the percentage of T_{SCM} plus T_{CM} was approximately 70% in the MK2206-treated CAR-T cells; however, it was only approximately 40% in the vehicle-treated CAR-T cells. On day 14, the CAR-T cells further differentiated into the terminal phase. The percentage of T_{SCM} plus T_{CM} significantly decreased and that of the effector memory T cells (T_{EM}) and terminally differentiated effector T cells (T_{TE}) significantly increased. However, the percentages of the memory T cell subsets (T_{SCM}, T_{CM} or T_{TE}) in the MK2206-treated CAR-T cells were significantly higher than those in the vehicle-treated CAR-T cell population (**Figure 3B**). Together, these data demonstrated that MK2206 treatment can inhibit T cell differentiation and generate CAR-T cell populations with memory-like characteristics.

As an important transcription regulator, active Forkhead box protein O1 (FoxO1) has been identified as a key promoter for memory $CD8^+$ T cell differentiation [26, 27]. Akt can activate FoxO1 through phosphorylating it at a series of 3 conserved serine and threonine residues, which causes cytosolic sequestration and prevents DNA binding [28, 29]. Inhibited Akt signalling in human T cells has been recently reported to generate a population of $CD62L^+$ T_{CM}- like cells through a FoxO1-dependent mechanism [30]. To test whether Akt inhibition results in the nuclear accumulation of FoxO1 in activated T cells, we performed western blot analysis with protein fractions isolated from the nucleus and compared them with those from the cytoplasm in T cells treated with of 2 μM MK2206 or the vehicle for 5 days. As shown in **Figure 3C** and **3D**, MK2206 treatment caused a significant increase in FoxO1 in the nucleus and a significant decrease in FoxO1 in the cytoplasm. To further confirm the differential subcellular localization of FoxO1 in activated T cells expanded with or without MK2206, we examined this protein in the T cell nucleus using confocal immunofluorescence imaging. Co-staining with Hoechst to define the boundary of the nucleus, we found that exposure to MK2206 resulted in a significant intranuclear localization of this transcription factor (**Figure 3E**). Therefore, MK2206 treatment generates EpCAM-CAR-T cell populations with memory-like characteristics through a FoxO1-dependent mechanism.

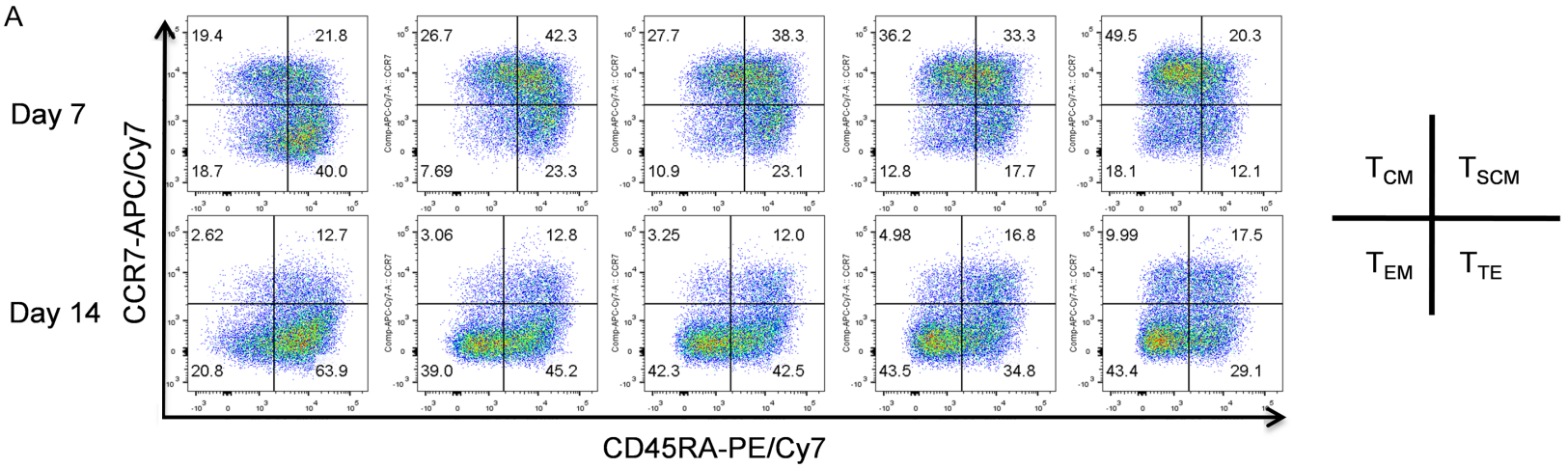
A
Day 7
Day 14
CCR7-APC/Cy7
CD45RA-PE/Cy7
19.4
21.8
18.7
40.0
26.7
42.3
7.69
23.3
27.7
38.3
10.9
23.1
36.2
33.3
12.8
17.7
49.5
20.3
18.1
12.1
2.62
12.7
20.8
63.9
3.06
12.8
39.0
45.2
3.25
12.0
42.3
42.5
4.98
16.8
43.5
34.8
9.99
17.5
43.4
29.1
TCM
TSCM
TEM
TTE

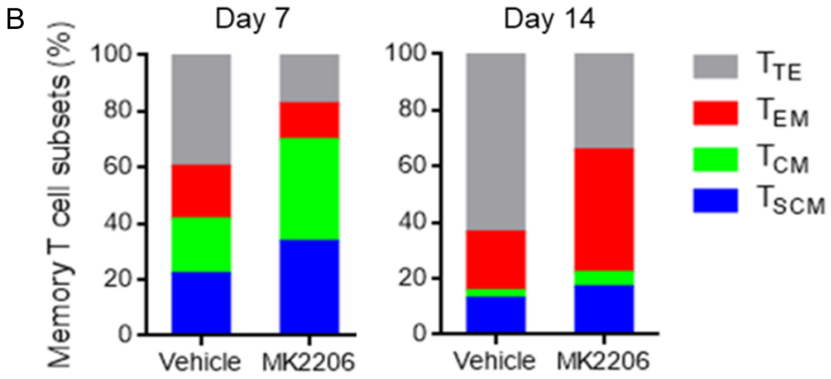
B
Day 7
Day 14
Memory T cell subsets (%)
100
80
60
40
20
0
Vehicle
MK2206
TTE
TEM
TCM
TSCM

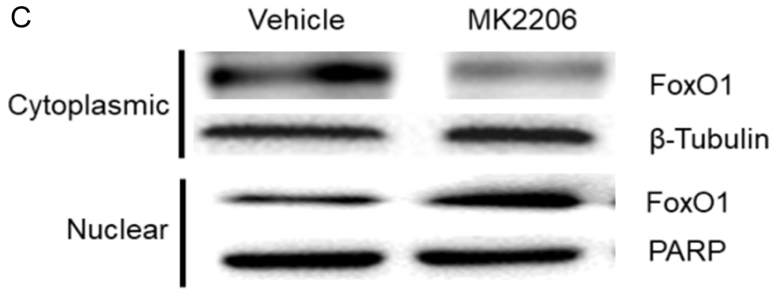
C
Vehicle
MK2206
Cytoplasmic
Nuclear
FoxO1
β-Tubulin
FoxO1
PARP

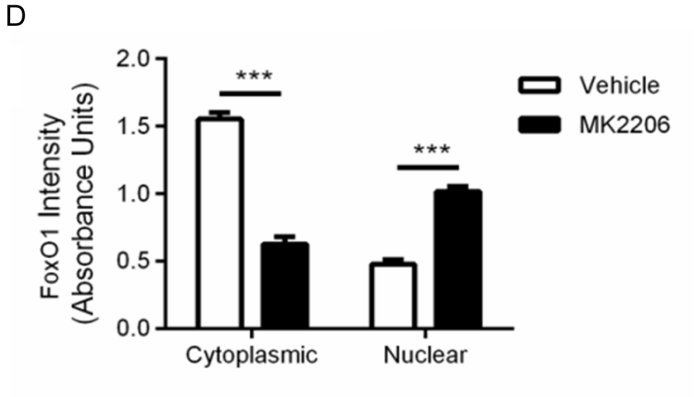
D
FoxO1 Intensity (Absorbance Units)
2.0
1.5
1.0
0.5
0.0
***
***
Vehicle
MK2206
Cytoplasmic
Nuclear

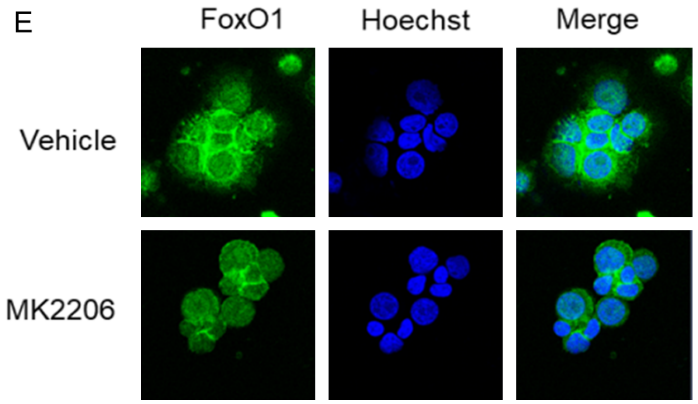
E
FoxO1
Hoechst
Merge
Vehicle
MK2206

Figure 3. MK2206 treatment generates EpCAM-CAR T cell populations with memory-like characteristics. (A, B) Representative data of flow cytometry (A) and comparative analysis results (B) of memory phenotype analysis of CAR-T cells. EpCAM-specific CAR-T cells were prepared as described in **Figure 1B** under treatment with the vehicle or 0.5~4 μM MK2206. CAR-T cells were collected on days 7 and 14. The memory phenotype of CAR-T cells was analysed by flow cytometry with anti-CCR7 and CD45RA antibodies. T_{SCM}, T memory stem cell; T_{CM}, central memory T cell; T_{EM}, effector memory T cell; T_{TE}, terminally differentiated effector T cells. (C) FoxO1 in the nucleus and cytoplasm was detected by western blot. PBMCs were activated with CD3/CD28 Dynabeads in medium containing 200 IU/mL rhIL-2 and vehicle or 2 μM MK2206. Five days later, the activated T cells were collected. The nuclear and cytoplasmic proteins were extracted using the nuclear and cytoplasmic protein extraction kit. FoxO1 in the nucleus and cytoplasm was analysed with an anti-FoxO1 antibody. PARP in the nucleus and β-tubulin in the cytoplasm were also detected as internal controls. (D) The quantitative analysis results of FoxO1 in the western blot analysis. The intensity of each strip was analyzed by ImageJ software. The average intensities of FoxO1 were standardized to β-Tubulin for cytoplasmic or PARP for nuclear. Shown are combined data from 3 independent experiments with mean ± SEM; ***P < 0.001. (E) The intracellular distribution of FoxO1 was analysed by immunofluorescence. Cell samples were prepared as described in (C). Five days after treatment, cells were collected and fixed with 4% paraformaldehyde. FoxO1 was probed with a primary anti-FoxO1 antibody and a secondary antibody. Hoechst 33342 counterstain was used to mask the nucleus. The images were taken with a confocal microscope.

MK2206 treatment does not suppress expansion ex vivo or cell-mediated cytotoxicity

As described above, we observed that inhibiting Akt with MK2206 treatment can enhance the CAR-positive expression rate and generate more memory-like CAR-T cells. However, Akt activation appears to be essential for proliferation, survival and effector functions of activated T cells [31, 32]. To confirm the effects of MK2206 treatment on the proliferation of EpCAM-CAR-T cells, we analysed cell proliferation. The CAR-T cells were prepared as described in **Figure 1B**. After removing anti-CD3/CD28 beads and MK2206, the cells were counted every day for 10 days. As shown in **Figure 4A** and **4B**, the MK2206 treatment does not inhibited the proliferation of CAR-T cells.

To assess the effects of MK2206 treatment on the functions of EpCAM-CAR-T cells, we used ELISA and a real-time cell assay (RTCA) to analyse the induction of cytokine release and cytotoxicity in the MK2206-treated EpCAM-CAR-T cells, respectively, upon co-culture with different target cells. EpCAM expression in human colon cancer cell lines and normal colon cell lines was detected by flow cytometry. Almost all cells of the human colon cancer cell lines HCT116 and SW620 are EpCAM-positive. However, no EpCAM is expressed in the human normal colon cell line FHC (**Figure 4C**). The results of ELISA showed that the levels of IFN-γ and granzyme-B released by the vehicle or MK2206-treated EpCAM-CAR-T cells were nearly equivalent; however, except the granzyme B level released by MK2206-treated EpCAM-CAR-T cells was higher than that released by the vehicle-treated EpCAM-CAR-T cells when co-cultured with SW620 cells (**Figure 4D**). The RTCA results also showed that there was no difference in killing ability between the vehicle and MK2206-treated EpCAM-CAR-T cells compared with the EpCAM-positive HCT116 and SW620 cells (**Figure 4E**). Together, these data demonstrated that MK2206 treatment does not suppress expanding ex vivo or ameliorate the cell-mediated cytotoxicity of EpCAM-CAR-T cells.

MK2206-treated EpCAM-CAR-T cells exhibited better antitumor efficacy and expansion in vivo

The principal aim of this study was to determine whether MK2206 promotes the generation of EpCAM-CAR-T cells with enhanced antitumor activity. First, we confirmed the efficacy of EpCAM-CAR-T cells prepared under a normal programme in vivo. The programme of the experiment is shown in **Figure 5A**. A total of 1×10^6 HCT116 cells were injected into the tail vein of NPG mice to establish a metastatic model of human colon cancer. On day 7, the mice were divided into 3 groups (n = 6). One group did not receive any treatment (untreated). The remaining 2 groups received empty vector-transduced T cells (Ctrl-T) or EpCAM-CAR-T cells (CAR-T) treatment. On day 14, a total of 50 μL blood was obtained from each mouse to detect the persistence of the infused human T cells in vivo. As shown in **Figure 5B** and **5C**, the infused Ctrl-T or EpCAM-CAR-T cells were detectable in the peripheral blood of the mice. The mice that received EpCAM-CAR-T cells showed significantly prolonged survival compared with those that received Ctrl-T cells

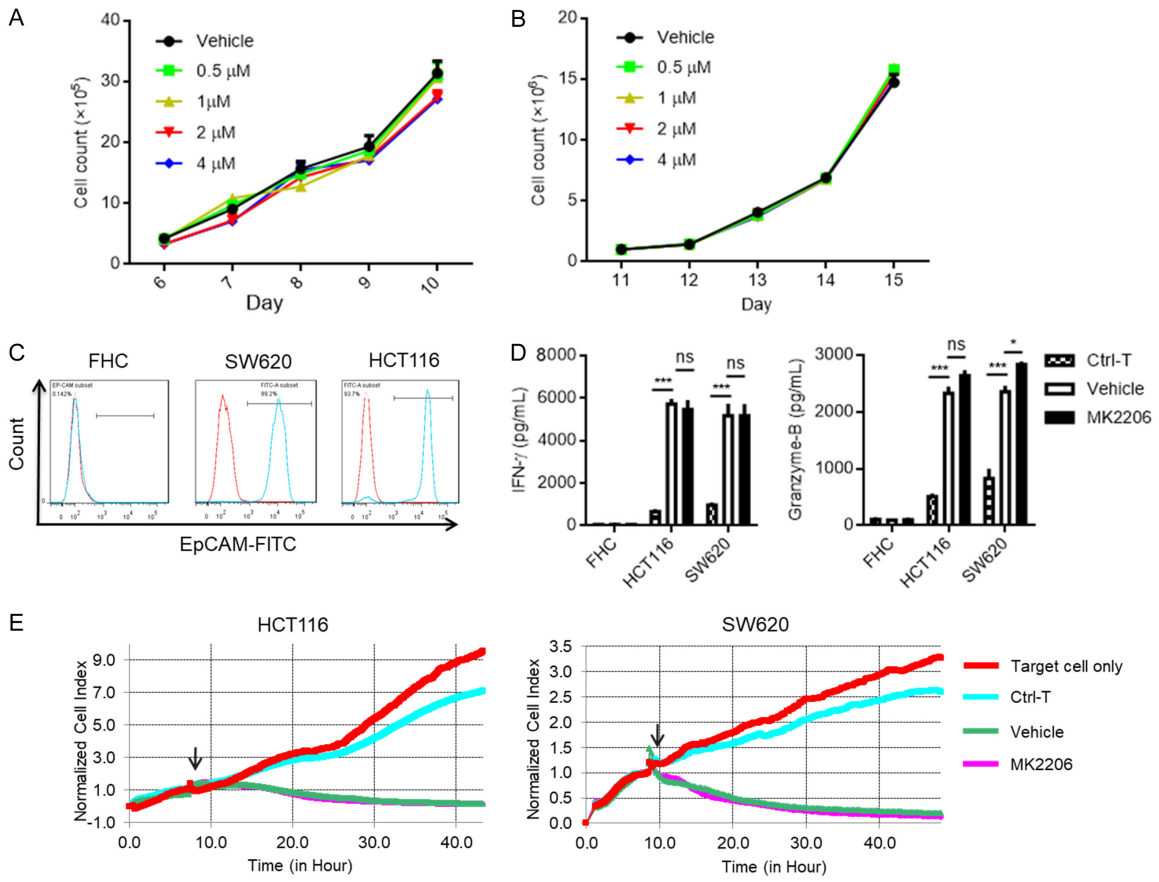

Figure 4. MK2206 treatment did not suppress the proliferation or ameliorate cell-mediated cytotoxicity. The EpCAM-CAR-T cells were prepared as described in **Figure 1B**. (A, B) Effects of MK2206 treatment on the proliferation of EpCAM-CAR-T cells. The cells were counted every day from day 6 to day 10 (A) by a Countess II Automated Cell Counter (Thermo Fisher). On Day 11, a total of 1 × 10^6 cells was taken from each group and continuously expanded. The cells were continuously counted until Day 15 (B). (C) The EpCAM expression in human normal colon cell lines and colon cancer cell lines were analysed by flow cytometry. The cell samples were incubated with an isotype control antibody (red open histogram) or an FITC-conjugated anti-EpCAM antibody (blue open histogram) and analysed by flow cytometry. (D) The release of cytokine was analysed by ELISA. The CAR-T cells treated with a vehicle or 2 μM MK2206 co-cultured with target cells at effector/target (E:T) = 1:1 for 24 h. The released IFN-γ and granzyme B in the supernatant were detected by ELISA. (E) The cytotoxicity was analysed by RTCA. The target cells were seeded at a density of 1 × 10^4 cells/well in an E-Plate and then transferred to the incubator. When the target cells reached a logarithmic growth phase, the empty vector-transduced T cells, the vehicle-treated CAR-T cells or the MK2206-treated CAR-T cells were added into the plate at E:T = 1 in duplicate. The proliferation of the target cells was continuously monitored by the RTCA machine. Ctrl-T, empty vector transduced T cell; Vehicle, vehicle-treated EpCAM-CAR-T cells; MK2206, MK2206-treated EpCAM-CAR-T cells. *P < 0.05; ***P < 0.001.

(P < 0.01) (**Figure 5D**). Therefore, EpCAM-specific CAR-T cells showed effective survival and therapeutic effects in vivo.

To further confirm the antitumor efficacy and expansion of MK2206-treated EpCAM-CAR-T cells in vivo, we established a metastatic model of human colon cancer with 1 × 10^6 $HCT116^{Luc+}$ cells were i.v. injected into the tail vein of the NPG mice. The protocol for the experiment is shown in **Figure 6A**. On day 7, the mice were divided into 2 groups (n = 5). One group was injected with 3 × 10^6 vehicle EpCAM-CAR-T cells (vehicle), and another group was injected with 3 × 10^6 MK2206-treated EpCAM-CAR-T cells (MK2206). On day 21, blood was drawn from the mice to detect the persistence and expansion of the infused CAR-T cells by flow cytometry. As shown in **Figure 6B** and **6C**, the MK2206-treated CAR-T cells showed a 2-fold expansion compared with the vehicle-treated CAR-T cells. On day 28, imaging of the mice was performed in vivo to confirm the therapeutic efficacy of the MK2206-treated EpCAM-CAR-T

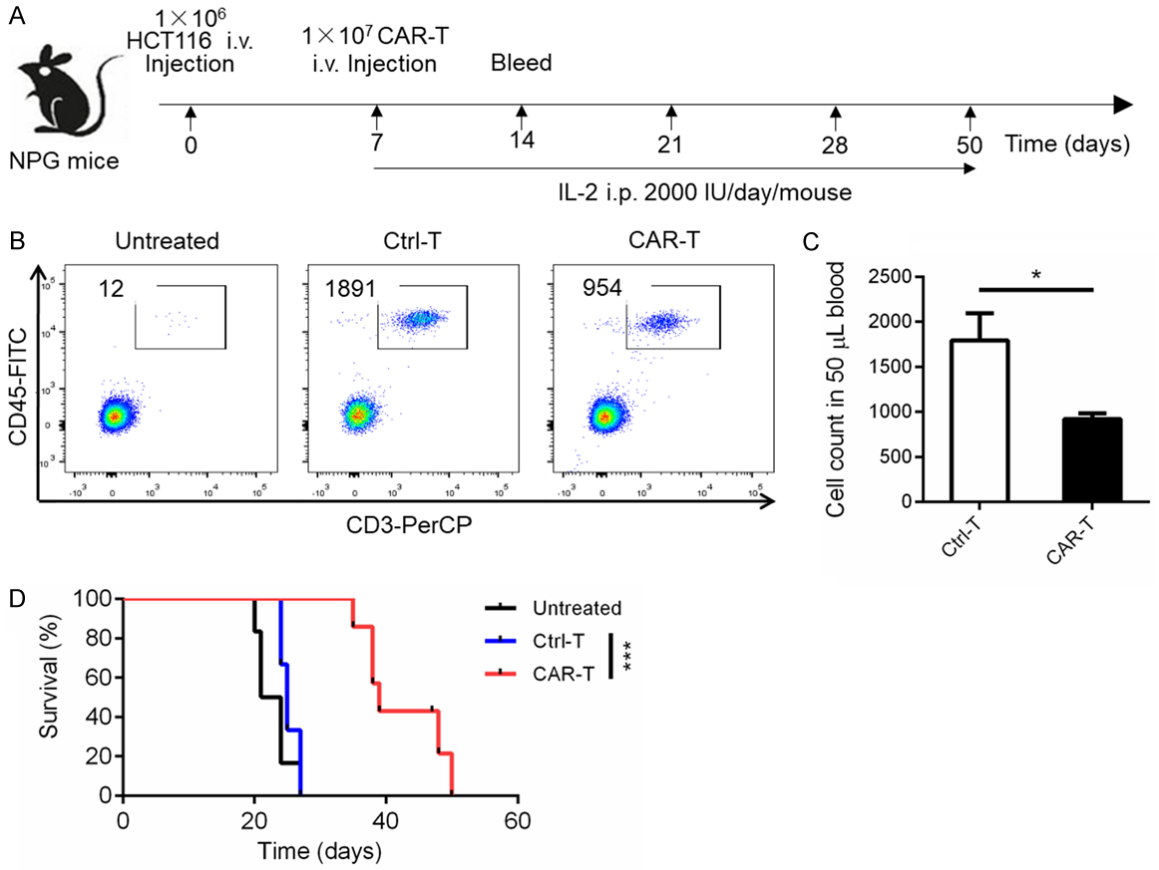

Figure 5. EpCAM-CAR-T treatment can prolong the survival of NPG mice with metastatic tumor from human colon cancer. (A) Schematic diagram showing the treatment programme of the mice. NPG mice were injected with 2 × 10^6 HCT116 cells via the tail vein to establish a metastasis model of human colon cancer. On day 7, the mice were randomly assigned into 3 groups (n = 6). The Ctrl-T group received 1 × 10^7 untransduced T cells. The CAR-T group received 1 × 10^7 EpCAM-CAR-T cells. All mice were intraperitoneally (i.p.) administered IL-2 (2000 IU/mouse) daily during the treatment. The experiment ended on day 50. (B, C) Results from the analysis of CAR-T cell persistence in vivo were based on flow cytometry. Blood (50 μL) was obtained from the tail vein on day 14. After red blood cell lysis, the cell samples were stained with anti-human CD45 and anti-CD3 antibodies and analysed by flow cytometry. Representative data (B) and statistical results (C) are shown. (D) Overall survival of the NPG mice bearing the established metastatic model of human colon cancer following Ctrl-T or EpCAM-CAR-T treatment. ***P < 0.001.

cells. The images taken in vivo (**Figure 6D**) and anatomical features of the dead mice (not shown) showed that metastases were mainly targeted to the kidneys. The results of fluorescence intensity analysis showed that the MK2206-treated EpCAM-CAR-T cells exhibited better antitumor efficacy than the CAR-T cells that received the vehicle treatment in vivo (**Figure 6E**). When all mice died (day 40), the survival of the mice was statistically analysed. As shown in **Figure 6F**, the mice that received MK2206-treated EpCAM-CAR-T cells survived longer than those that received the vehicle-treated EpCAM-CAR-T cells. Together, these data demonstrated that MK2206-treated EpCAM-CAR-T cells exhibited better antitumor efficacy and reduced tumor expansion in vivo.

Discussion

Effective adoptive CAR-T cell therapy against cancer relies on the formation of T cells with a high CAR-positive expression rate, long-term survival and memory phenotype, which can self-renew and differentiate into potent effector T cells. Some strategies have been used to produce CAR-T cells with a better immune phenotype and function, such as using RetroNectin to activate and expand T cells [33, 34], supplementing with cytokine cocktails during expansion ex vivo [34-36], and inhibiting the intrinsic signalling pathway by chemical small molecules [37]. However, few means have been reported to increase the CAR-positive expression rate or enhance the memory phenotype of the CAR-T

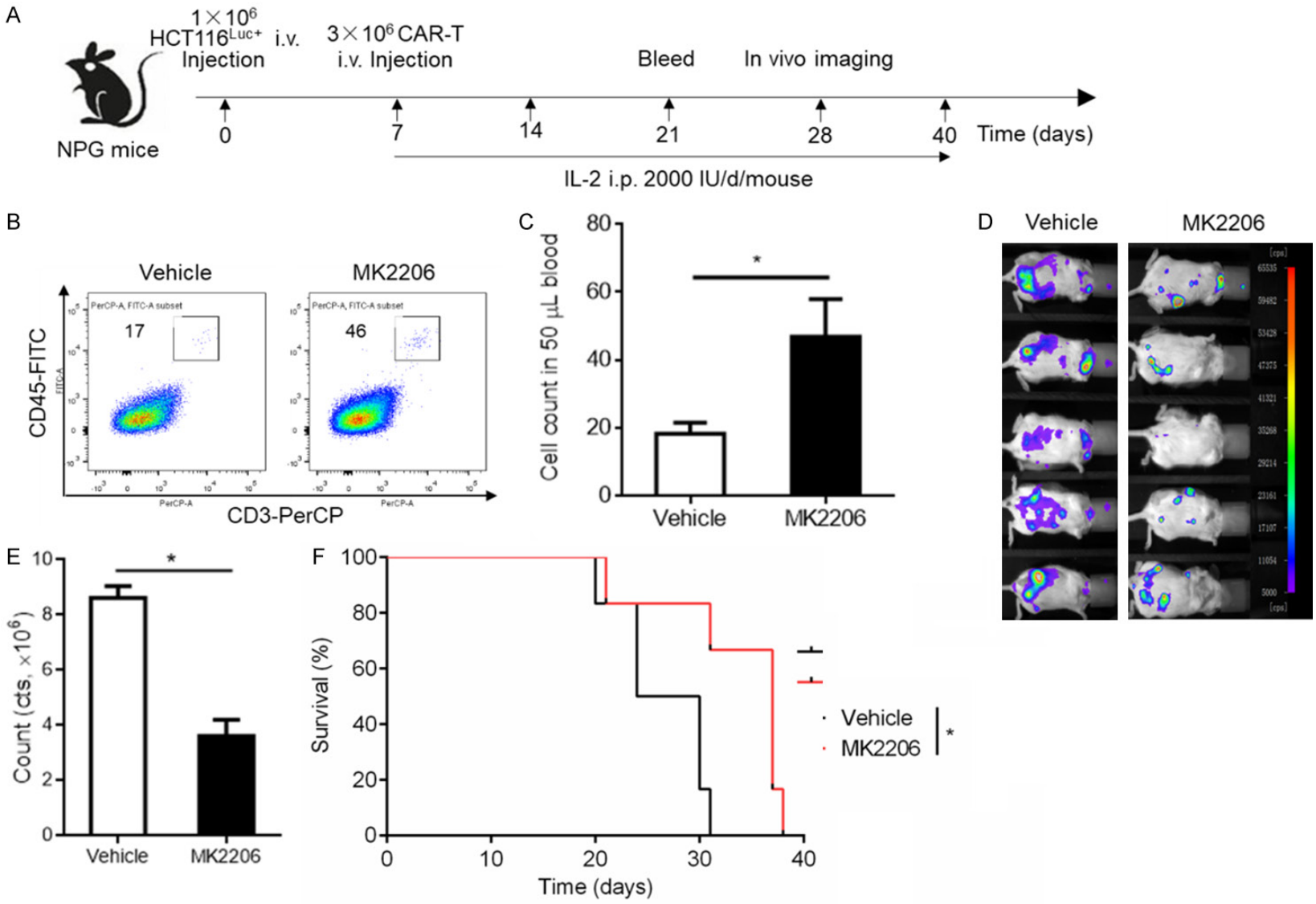

Figure 6. MK2206-treated EpCAM-CAR-T cells exhibited better antitumor efficacy against a metastatic model of human colon cancer established in NPG mice. (A) Schematic diagram showing the treatment programme of the mice. The NPG mice were injected with 2 × 10^6 HCT116^{luc+} cells via the tail vein to establish a metastasis model of human colon cancer. On day 7, the mice were randomly assigned to 2 groups (n = 5). The vehicle group received 3 × 10^6 vehicle-treated EpCAM-CAR-T cells. The MK2206 group received 3 × 10^6 2 μM MK2206-treated EpCAM-CAR-T cells. All mice were intraperitoneally (i.p.) administered IL-2 (2000 IU/mouse) daily during the treatment. The experiment ended on day 40. (B, C) Results from the analysis of CAR-T cell persistence in vivo by flow cytometry. Blood (50 μL)

was obtained from the tail vein on day 21. After red blood cell lysis, the cell samples were stained with anti-human CD45 and anti-CD3 antibodies and analysed by flow cytometry. Representative data (B) and statistical results (C) are shown. (D, E) The therapeutic efficacy was evaluated through luminescence imaging with an IVIS system. Luminescence images (D) and quantitative results (E) of the tumor luminescence intensity showed the tumor burden on day 28. (F) The overall survival of the NPG mice bearing the established metastatic model of human colon cancer following injection of the vehicle or MK2206-treated EpCAM-CAR-T cells. *P < 0.05.

cells simultaneously. Although RetroNectin is well established as an adjuvant for improved retroviral transduction and has also been reported to have the ability to activate and enrich less-differentiated T cells [34], a recent report showed that activation with RetroNectin decreased the transduction efficacy of CAR-T cells [33].

Akt inhibition with Akt inhibitor VIII during CAR-T expansion has been reported to enhance the memory phenotype and in vivo therapeutic efficacy of CAR-T cells [38]. Herein, we demonstrated the cost-effective and translatable strategy of adding an Akt inhibitor (MK2206) at the initial stage of CAR-T preparation to produce CAR-T cells with an enhanced CAR-positive expression rate and memory phenotype. Importantly, this critical strategy successfully uncoupled the process of T cell expansion from phenotypic, functional, and metabolic maturation, resulting in CAR-T cells with improved antitumor efficacy in vivo.

Akt activation has been reported to be essential for the proliferation, survival and effector functions of activated T cells [31, 32]. To confirm the concentration of MK2206 required for significant inhibition of T cell differentiation and for the enhancement of the CAR-positive expression rate without suppressing proliferation and the effector functions of CAR-T cells, we treated the CAR-T cells with MK2206 at different concentrations (0.5-4 μM) first during the activation of PBMCs and finally to the end of CAR-T cell expansion over a total of approximately 12 days. We found that long-term treatment with MK2206 significantly inhibited the expansion and impaired the viability of the CAR-T cells, especially at a concentration of 4 μM (data not shown). Therefore, to avoid negatively affecting the expansion and effector functions of the CAR-T cells, we chose the protocol in which 2 μM MK2206 was used to treat the cells for 5 days at the initial stage of CAR-T cell preparation.

In this study, we found that inhibiting Akt phosphorylation with MK2206 enhanced the CAR-positive expression rate of the EpCAM-CAR-T cell population. Because the LDL receptor is the major membrane protein that mediates lentivirus infection of T cells, we confirmed that MK2206 treatment enhanced LDL-R expression on the surface of activated T cells. However, the results of flow cytometry showed that MK2206 treatment not only failed to increase LDL-R expression on the surface of activated T cells it also reduced it. Therefore, MK2206 does not increase the positive rate of CAR by increasing the expression of LDL-R on the surface of activated T cells. The infection efficiency of HIV has been previously reported to be modulated by the state of the host cell cycle. Cell cycle arrest in G2/M can promote the early stages of infection by HIV [3, 4]. In addition, extended G0/G1 and G2/M phases have been positively correlated with the gene expression efficiency of infected lentivirus [5-7]. Therefore, we speculated that the increase in the CAR-positive expression rate may be due to MK2206-induced changes in the cell cycle. The results of our cell cycle analysis showed that MK2206 treatment can prolong the G0/G1 and G2/M phases in activated T cells. Based on these results, MK2206 may enhance the CAR-positive expression rate by prolonging the G0/G1 and G2/M phases of activated T cells. However, the specific mechanisms need to be further studied.

We demonstrated that MK2206 significantly inhibits T cell differentiation during expansion, resulting in an increased proportion of early differentiated T cells in the final CAR-T cell product. Although MK2206-treated EpCAM-CAR-T cells did not show enhanced killing effects on EpCAM-positive colon cancer cells in vitro at E:T = 1:1, they showed greater expansion and therapeutic effects against a metastasis model of human colon cancer in immune deficient NPG mice in vivo. The underlying mechanisms may be related to changes in the altered intracellular localization of FoxO1, a key promoter of T cell differentiation [26, 27].

Our current studies demonstrate that the Akt inhibitor (MK2206) does not suppress EpCAM-

CAR-T cell expansion, viability, or effector functions but promotes the generation of memory EpCAM-CAR-T cells with enhanced CAR-positive expression rates and greater antitumor activity in vivo. These results support the use of MK2206 for further improved CAR-T cell therapy.

Acknowledgements

This work was supported by grants from the National Science Foundation of China (81773253, 81872488), Jiangsu Province Social Development Projects (SBE2018740637, BE2016643), the Natural Science Key Project of Jiangsu Provincial Education Department (17KJA320011), the 333 Project of Jiangsu Province (BRA2016398), the Qing Lan Project of Jiangsu Province, and Jiangsu Provincial Key Medical Discipline, the Project of Invigorating Health care through Science, Technology and Education (NO.ZDXKA2016014).

Disclosure of conflict of interest

None.

Address correspondence to: Dr. Junnian Zheng, Cancer Institute, Xuzhou Medical University, Xuzhou 221002, Jiangsu, P. R. China. Tel: +86-516-8558-2530; E-mail: jnzheng@xzhmu.edu.cn

References

[1] Zhang Q, Li H, Yang J, Li L, Zhang B, Li J and Zheng J. Strategies to improve the clinical performance of chimeric antigen receptor-modified T cells for cancer. Curr Gene Ther 2013; 13: 65-70.

[2] Xu J, Tian K, Zhang H, Li L, Liu H, Liu J, Zhang Q and Zheng J. Chimeric antigen receptor-T cell therapy for solid tumors require new clinical regimens. Expert Rev Anticancer Ther 2017; 17: 1099-1106.

[3] Groschel B and Bushman F. Cell cycle arrest in G2/M promotes early steps of infection by human immunodeficiency virus. J Virol 2005; 79: 5695-5704.

[4] Jowett JB, Planelles V, Poon B, Shah NP, Chen ML and Chen IS. The human immunodeficiency virus type 1 vpr gene arrests infected T cells in the G2 + M phase of the cell cycle. J Virol 1995; 69: 6304-6313.

[5] Wang XP and Lewis DE. CD86 expression correlates with amounts of HIV produced by macrophages in vitro. J Leukoc Biol 2001; 69: 405-413.

[6] Korin YD and Zack JA. Nonproductive human immunodeficiency virus type 1 infection in nucleoside-treated G0 lymphocytes. J Virol 1999; 73: 6526-6532.

[7] Kundu M, Sharma S, De Luca A, Giordano A, Rappaport J, Khalili K and Amini S. HIV-1 Tat elongates the G1 phase and indirectly promotes HIV-1 gene expression in cells of glial origin. J Biol Chem 1998; 273: 8130-8136.

[8] Wu H, Li L, Ai Z, Yin J and Chen L. Pristimerin induces apoptosis of oral squamous cell carcinoma cells via G1 phase arrest and MAPK/Erk1/2 and Akt signaling inhibition. Oncol Lett 2019; 17: 3017-3025.

[9] Cui T, Yang L, Ma Y, Petersen I and Chen Y. Desmocollin 3 has a tumor suppressive activity through inhibition of AKT pathway in colorectal cancer. Exp Cell Res 2019; 378: 124-130.

[10] Zhao S, Wang L, Zhang C, Deng Y, Zhao B, Ren Y, Fu Y and Meng X. Inhibitor of growth 3 induces cell death by regulating cell proliferation, apoptosis and cell cycle arrest by blocking the PI3K/AKT pathway. Cancer Gene Ther 2018; 25: 240-247.

[11] Xiao W, Li B, Sun X, Yu D, Xie Y, Wu H, Chang S, Zhou Y, Wang H, Lan X, Xu Z, Shi J and Zhu W. DCZ3301, a novel aryl-guanidino inhibitor, induces cell apoptosis and cell cycle arrest via suppressing the PI3K/AKT pathway in T-cell leukemia/lymphoma. Acta Biochim Biophys Sin (Shanghai) 2018; 50: 643-650.

[12] Gattinoni L, Klebanoff CA, Palmer DC, Wrzesinski C, Kerstann K, Yu Z, Finkelstein SE, Theoret MR, Rosenberg SA and Restifo NP. Acquisition of full effector function in vitro paradoxically impairs the in vivo antitumor efficacy of adoptively transferred CD8+ T cells. J Clin Invest 2005; 115: 1616-1626.

[13] Louis CU, Savoldo B, Dotti G, Pule M, Yvon E, Myers GD, Rossig C, Russell HV, Diouf O, Liu E, Liu H, Wu MF, Gee AP, Mei Z, Rooney CM, Heslop HE and Brenner MK. Antitumor activity and long-term fate of chimeric antigen receptor-positive T cells in patients with neuroblastoma. Blood 2011; 118: 6050-6056.

[14] Rosenberg SA, Yang JC, Sherry RM, Kammula US, Hughes MS, Phan GQ, Citrin DE, Restifo NP, Robbins PF, Wunderlich JR, Morton KE, Laurencot CM, Steinberg SM, White DE and Dudley ME. Durable complete responses in heavily pretreated patients with metastatic melanoma using T-cell transfer immunotherapy. Clin Cancer Res 2011; 17: 4550-4557.

[15] Kim EH and Suresh M. Role of PI3K/Akt signaling in memory CD8 T cell differentiation. Front Immunol 2013; 4: 20.

[16] Yoo JK, Cho JH, Lee SW and Sung YC. IL-12 provides proliferation and survival signals to murine CD4+ T cells through phosphatidylinositol

3-kinase/Akt signaling pathway. J Immunol 2002; 169: 3637-3643.
[17] Kim EH, Sullivan JA, Plisch EH, Tejera MM, Jatzek A, Choi KY and Suresh M. Signal integration by Akt regulates CD8 T cell effector and memory differentiation. J Immunol 2012; 188: 4305-4314.
[18] Zhang Q, Zhang H, Ding J, Liu H, Li H, Li H, Lu M, Miao Y, Li L and Zheng J. Combination therapy with EpCAM-CAR-NK-92 cells and regorafenib against human colorectal cancer models. J Immunol Res 2018; 2018: 4263520.
[19] Cao J, Wang G, Cheng H, Wei C, Qi K, Sang W, Zhenyu L, Shi M, Li H, Qiao J, Pan B, Zhao J, Wu Q, Zeng L, Niu M, Jing G, Zheng J and Xu K. Potent anti-leukemia activities of humanized CD19-targeted Chimeric antigen receptor T (CAR-T) cells in patients with relapsed/refractory acute lymphoblastic leukemia. Am J Hematol 2018; 93: 851-858.
[20] Kochenderfer JN, Somerville RPT, Lu T, Shi V, Bot A, Rossi J, Xue A, Goff SL, Yang JC, Sherry RM, Klebanoff CA, Kammula US, Sherman M, Perez A, Yuan CM, Feldman T, Friedberg JW, Roschewski MJ, Feldman SA, McIntyre L, Toomey MA and Rosenberg SA. Lymphoma remissions caused by Anti-CD19 chimeric antigen receptor T cells are associated with high serum interleukin-15 levels. J Clin Oncol 2017; 35: 1803-1813.
[21] Locke FL, Neelapu SS, Bartlett NL, Siddiqi T, Chavez JC, Hosing CM, Ghobadi A, Budde LE, Bot A, Rossi JM, Jiang Y, Xue AX, Elias M, Aycock J, Wiezorek J and Go WY. Phase 1 results of ZUMA-1: a multicenter study of KTE-C19 Anti-CD19 CAR T cell therapy in refractory aggressive lymphoma. Mol Ther 2017; 25: 285-295.
[22] Acevedo ML, Garcia-de Gracia F, Miranda-Cardenas C, Soto-Rifo R, Aguayo F and Leon O. Differences in the internalization of self-inactivating VSVG-pseudotyped murine leukemia virus-based vectors in human and murine cells. J Virol Methods 2018; 255: 14-22.
[23] Klebanoff CA, Gattinoni L and Restifo NP. Sorting through subsets: which T-cell populations mediate highly effective adoptive immunotherapy? J Immunother 2012; 35: 651-660.
[24] Li YX and Kurlander RJ. Comparison of anti-CD3 and anti-CD28-coated beads with soluble anti-CD3 for expanding human T cells: differing impact on CD8 T cell phenotype and responsiveness to restimulation. J Transl Med 2010; 8: 104.
[25] Macintyre AN, Finlay D, Preston G, Sinclair LV, Waugh CM, Tamas P, Feijoo C, Okkenhaug K and Cantrell DA. Protein kinase b controls transcriptional programs that direct cytotoxic T cell fate but is dispensable for T cell metabolism. Immunity 2011; 34: 224-236.
[26] Hess Michelini R, Doedens AL, Goldrath AW and Hedrick SM. Differentiation of CD8 memory T cells depends on Foxo1. J Exp Med 2013; 210: 1189-1200.
[27] Rao RR, Li Q, Gubbels Bupp MR and Shrikant PA. Transcription factor Foxo1 represses T-bet-mediated effector functions and promotes memory CD8(+) T cell differentiation. Immunity 2012; 36: 374-387.
[28] Rena G, Guo S, Cichy SC, Unterman TG and Cohen P. Phosphorylation of the transcription factor forkhead family member FKHR by protein kinase B. J Biol Chem 1999; 274: 17179-17183.
[29] Greer EL and Brunet A. FOXO transcription factors at the interface between longevity and tumor suppression. Oncogene 2005; 24: 7410-7425.
[30] Klebanoff CA, Crompton JG, Leonardi AJ, Yamamoto TN, Chandran SS, Eil RL, Sukumar M, Vodnala SK, Hu J, Ji Y, Clever D, Black MA, Gurusamy D, Kruhlak MJ, Jin P, Stroncek DF, Gattinoni L, Feldman SA and Restifo NP. Inhibition of AKT signaling uncouples T cell differentiation from expansion for receptor-engineered adoptive immunotherapy. JCI Insight 2017; 2.
[31] Cantrell DA. T-cell antigen receptor signal transduction. Immunology 2002; 105: 369-374.
[32] Kane LP and Weiss A. The PI-3 kinase/Akt pathway and T cell activation: pleiotropic pathways downstream of PIP3. Immunol Rev 2003; 192: 7-20.
[33] Stock S, Hoffmann JM, Schubert ML, Wang L, Wang S, Gong W, Neuber B, Gern U, Schmitt A, Muller-Tidow C, Dreger P, Schmitt M and Sellner L. Influence of retronectin-mediated T-cell activation on expansion and phenotype of CD19-specific chimeric antigen receptor T cells. Hum Gene Ther 2018; 29: 1167-1182.
[34] Gargett T and Brown MP. Different cytokine and stimulation conditions influence the expansion and immune phenotype of third-generation chimeric antigen receptor T cells specific for tumor antigen GD2. Cytotherapy 2015; 17: 487-495.
[35] Gargett T, Truong N, Ebert LM, Yu W and Brown MP. Optimization of manufacturing conditions for chimeric antigen receptor T cells to favor cells with a central memory phenotype. Cytotherapy 2019; 21: 593-602.
[36] Xu XJ, Song DG, Poussin M, Ye Q, Sharma P, Rodriguez-Garcia A, Tang YM and Powell DJ. Multiparameter comparative analysis reveals differential impacts of various cytokines on

CART cell phenotype and function ex vivo and in vivo. Oncotarget 2016; 7: 82354-82368.

[37] Kagoya Y, Nakatsugawa M, Yamashita Y, Ochi T, Guo T, Anczurowski M, Saso K, Butler MO, Arrowsmith CH and Hirano N. BET bromodomain inhibition enhances T cell persistence and function in adoptive immunotherapy models. J Clin Invest 2016; 126: 3479-3494.

[38] Urak R, Walter M, Lim L, Wong CW, Budde LE, Thomas S, Forman SJ and Wang X. Ex vivo Akt inhibition promotes the generation of potent CD19CAR T cells for adoptive immunotherapy. J Immunother Cancer 2017; 5: 26.